Bioorganic & Medicinal Chemistry Letters 23 (2013) 1238–1244

Contents lists available at SciVerse ScienceDirect

Bioorganic & Medicinal Chemistry Letters

journal homepage: www.elsevier.com/locate/bmcl

Inhibiting NF-κB-inducing kinase (NIK): Discovery, structure-based design, synthesis, structure–activity relationship, and co-crystal structures

Kexue Li *, Lawrence R. McGee, Ben Fisher, Athena Sudom, Jinsong Liu, Steven M. Rubenstein, Mohmed K. Anwer, Timothy D. Cushing, Youngsook Shin, Merrill Ayres, Fei Lee, John Eksterowicz, Paul Faulder, Bohdan Waszkowycz, Olga Plotnikova, Ellyn Farrelly, Shou-Hua Xiao, Guoqing Chen, Zhulun Wang

Amgen Inc., 1120 Veterans Boulevard, South San Francisco, CA 94080, USA

ARTICLE INFO

Article history:
Received 16 November 2012
Revised 18 December 2012
Accepted 2 January 2013
Available online 11 January 2013

Keywords:
NIK
Nuclear factor (NF)-κB
p100 processing
2-Aminopyrimidine

ABSTRACT

The discovery, structure-based design, synthesis, and optimization of NIK inhibitors are described. Our work began with an HTS hit, imidazopyridinyl pyrimidinamine **1**. We utilized homology modeling and conformational analysis to optimize the indole scaffold leading to the discovery of novel and potent conformationally constrained inhibitors such as compounds **25** and **28**. Compounds **25** and **31** were co-crystallized with NIK kinase domain to provide structural insights.

Nuclear factor (NF)-κB is a group of conserved eukaryotic transcription factors that regulates the expression of genes critical for both innate and adaptive immune responses.[1] As a member of the mitogen-activated protein kinase kinase kinase (MAP3K) family, NF-κB-inducing kinase (NIK) is a serine/threonine protein kinase essential for the activation of a second major NF-κB (NF-κB2) pathway.[1–3] NIK regulates the NF-κB2 activation by promoting proteolytic processing of the NF-κB2 precursor p100 to its active form p52[4] and the generation of NF-κB heterodimers such as p52:RelB, that bind DNA and activate the transcription of targeted genes. p100 processing or NF-B2 activation is defective in the absence of functional NIK.[2,3]

NIK-dependent NF-κB2 activation plays a decisive role in signaling the biological activity of both BAFF/BAFF-R[5–8] and (LTα/β2)/LTβ-R pathways.[2,3,9] BAFF-R signaling is instrumental in the development and maturation of peripheral B cells. Abnormal B cell activity caused by excess BAFF is associated with the etiology of autoimmunity[10] and B cell lymphomas.[11–14] LTβ-R signaling directs secondary lymphoid organogenesis, which often is a hallmark for the progression of chronic inflammation and certain autoimmune conditions.[15] NIK is also required in the signaling pathways elicited by several other TNF-family cytokines, including CD27L, CD40L, TWEAK, and RANKL (receptor activator of NF-κB ligand),[16] which are also associated with autoimmunity, B cell-driven cancers, and osteoporosis.[17] Treatment with soluble receptors for BAFF/LTβ/TWEAK significantly reduces and even prevents disease symptoms in mouse models of systemic lupus erythematosus (SLE) and rheumatoid arthritis (RA).[18,19]

Thus, a small-molecule inhibitor specific for NIK may provide a novel approach in the intervention of NF-κB2 signaling and modulation of the immune system.

High-throughput screening[20] of our small-molecule compound library utilizing a truncated form of NIK (tNIK) containing only the catalytic domain[21] resulted in the identification of imidazopyridinyl pyrimidinamine **1** (Fig. 1) as a submicromolar NIK inhibitor. In a cell-based assay[22] using human HT29 cells, compound **1** imparted weak inhibition of LTα/β2 induced p100 processing to NF-κB2 (p52) in a dose-dependent manner with an IC_{50} of 16 μM.

Structurally, compound **1** resembles the guanidine-based indole alkaloids meridianins (Fig. 1), a class of marine natural products whose synthesis has already been described.[23] In our initial SAR study, various isosteric replacements of the imidazopyridine such as benzimidazole, indoles and indoline were evaluated to assess the impact on NIK inhibition by scaffold modification (Table 1). Benzimidazoles **3** and **4** and N-linked indoline **10** are less active

* Corresponding author. Tel.: +1 650 244 2173.
E-mail address: kli@amgen.com (K. Li).

0960-894X/$ - see front matter © 2013 Elsevier Ltd. All rights reserved.
http://dx.doi.org/10.1016/j.bmcl.2013.01.012

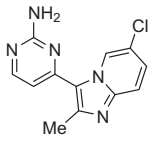

1
(HTS Hit)
NIK_CLA_IC_{50} 0.6 μM
NIK_HT29_IC_{50} 16 μM

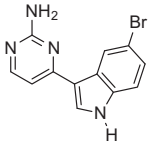

Meridianin C

Figure 1. NIK HTS hit and meridianin C.

Table 1
SAR of 4-substituted-2-aminopyrimidines

Compound	R	R^1	R^2	NIK_CLA_IC_{50}^{20} (μM)
1	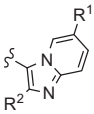	Cl	Me	0.60
2		Br	H	0.19 (n = 1)
3	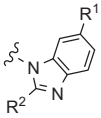	Cl	Me	4.0
4		Cl	H	0.31 (n = 1)
5	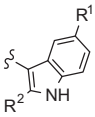	Cl	Me	0.30
6		Cl	H	0.15
7	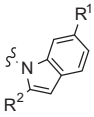	Cl	H	0.076
8		Br	H	0.089
9		CN	H	0.063 (n = 1)
10	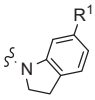	Br		0.55

than the corresponding imidazopyridines **1** and **2** and indoles **5**–**9**. Indoles are better tolerated than imidazopyridines. N-Linked indoles **7**–**9** are more active than the C-linked indoles **5** and **6**. Noteworthy is that compounds **7**–**9** with the single-point variations Cl, Br, and CN at R on the N-linked indoles exhibit similar potency.

Next, we turned our attention to examine the electronic effect of the substitution off the phenyl ring. Due to the afore-mentioned structural resemblance to the natural indole alkaloids, the 3-indolyl scaffold was studied. Evaluation of substitutions (Table 2) at position 5 revealed that electron-withdrawing groups are better tolerated. The cyano group furnished the most active compound, **14**, among these analogs.

A similar SAR trend was observed with the imidazopyridine scaffold (Table 3) where the inhibitory activity appeared very sensitive to removal or replacement of the chlorine atom at position 6 with a moderately electron-donating methyl group. For example, compounds **15** and **18** become significantly less active compared with compound **1**. Compound **2**, a des-Me analog of compound **1** is more active. Moving substitution to position 7 or 8 such as compounds **16** and **17** causes significant loss of activity.

Table 2
SAR at position 5 of the 3-indole scaffold

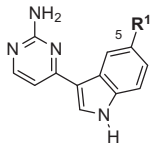

Compound	R^1	NIK_CLA_IC_{50}^{20} (μM)
6	Cl	0.15
11	H	41 (n = 1)
12	F	1.8
13	OMe	24 (n = 1)
14	CN	0.063

Table 3
SAR of the imidazopyridine scaffold

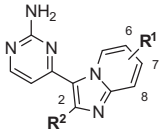

Compound	R^1	R^2	NIK_CLA_IC_{50}^{20} (μM)
1	6-Cl	Me	0.60
15	6-Me	Me	42 (n = 1)
16	7-Me	Me	>80 (n = 1)
17	8-Me	Me	>80 (n = 1)
18	H	Me	>80 (n = 1)
2	6-Br	H	0.19 (n = 1)

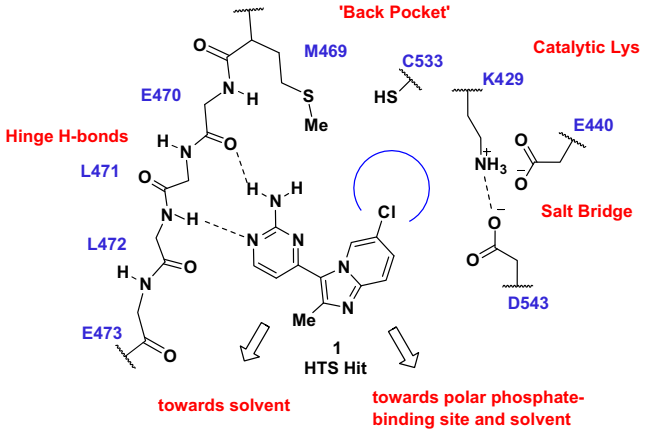

Figure 2. A NIK homology model.

To further guide our SAR effort, a NIK homology model (Fig. 2) was built upon the crystal structure of a human cell cycle checkpoint kinase 1 (CHK1) (PDB code: 1NVR.pdb)[24] that shares 31% sequence identity and 49% similarity in the catalytic domain with NIK. In this model, the binding site is a deep narrow pocket with the aminopyrimidine engaged in hinge interactions. The side chains of M469, C533 and the alkyl portion of K429 appear to restrict access to a back pocket.

One of the two possible binding modes of compound **1**, conformation **A** (Fig. 3), is shown docked in Figure 2, with the amino group in a hydrogen bonding interaction with the carbonyl oxygen of E470. In an alternate binding mode, conformation **B** (Fig. 3), the

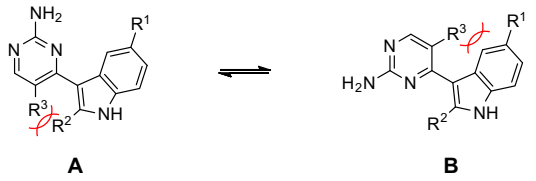

Figure 3. Conformational analysis.

aminopyrimidine ring flips around the biaryl bond so that the amino hydrogen interacts with the carbonyl oxygen of L472. Biaryl compounds such as compound **1** exist in equilibrium between different conformations like **A** and **B** (Fig. 3) from rotation about the biaryl bond, and the relative energies of these conformations can vary depending on the surrounding *ortho* substitutions. They tend to adopt certain dihedral angles in silico while the biaryl rings are forced to become more coplanar when binding to the protein.

The SAR around the 4-(5-chloroindol-3-yl)pyrimidin-2-amine scaffold (Table 4) provided key evidence in the elucidation of the preferred binding mode of our small molecule NIK inhibitors. Compared to compound **6**, methyl groups at R2 or R3 are individually well tolerated (compounds **5** and **19**). However, methyl groups at both R2 and R3 simultaneously are not well tolerated (compound **20**). Molecular mechanics calculations[25] show that the low energy conformation in solution for each compound is twisted about the biaryl bond to some extent (Table 4). The energy penalty for rotation around this bond to an angle appropriate for binding (~10° as for **25** in its binding conformation in Fig. 4) is modest, <2 kcal/mol for compounds **6**, **19** and **5**, but is >14 kcal/mol for **20** due to the significant steric clash resulting from the R2 and R3 methyl groups. These differences in the energy penalty can explain the lack of potency for **20** but do not allow a clear distinction between binding modes **A** and **B**. Constrained analogs **21** and **22** were synthesized to probe the question of the preferred orientation of the aminopyrimidine moiety in the ATP pocket. The result was a 37-fold difference in potency, favoring **21**. The loss of activity for compound **20** and the fact that the conformationally constrained analog **21** is much more active than compound **22** suggests that conformation **A** is the preferred binding mode.

To investigate the effect of ring size, the six- and eight-membered ring homologs, **23** and **24** (Table 5), were prepared and found to be less active than the seven-membered **21**.

With our SAR study unfolding, co-crystallization of the NIK kinase domain with the bromo analog **25** (Table 6) of compound **21** was achieved furnishing the first NIK-inhibitor co-crystal structure[26] (Fig. 4) known at that time. The aminopyrimidine motif of the inhibitor forms typical kinase hinge hydrogen bonding interactions with the protein backbone while the other parts of the molecule engage in numerous van der Waals (VDW) contacts with the protein. The bromine atom, in particular, points towards the pocket in the back and makes VDW contacts with the gatekeeper M469 and the catalytic K429. Interestingly, the co-crystal structure reveals that NIK has a large back pocket where three water molecules are observed, indicating the polar nature within the pocket

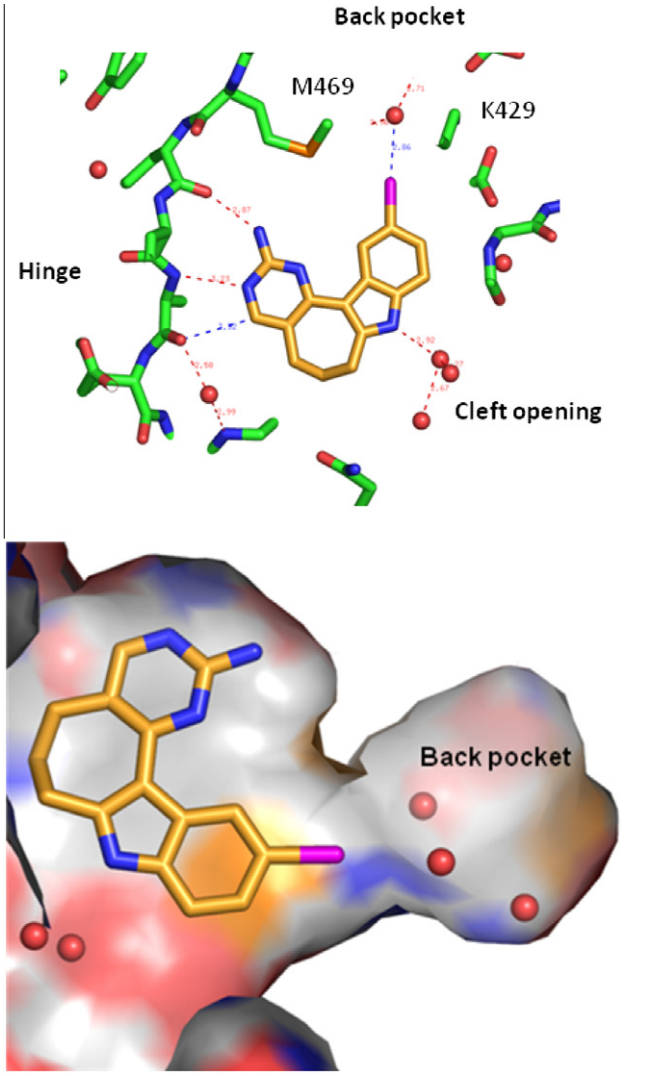

Figure 4. The co-crystal structure of NIK with compound **25** at a resolution of 2.4 Å (PDB code: 4IDT.pdb).

Table 4
SAR of 4-(1*H*-5-chloroindol-3-yl)pyrimidin-2-amine

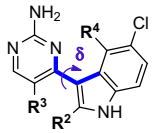

Compound	R^2	R^3	R^4	NIK_CLA_IC_{50}[20] (μM)	δ (Dihedral angle, calcd) (°)
6	H	H	H	0.15	22
19	H	Me	H	0.11	50
5	Me	H	H	0.30	41
20	Me	Me	H	30	66
21	$-(CH_2)_3-$		H	0.070	27 (Constrained)
22	H	$-(CH_2)_2-$		2.6 (n = 1)	159 (Constrained)

Table 5
Conformationally constrained indole analogs

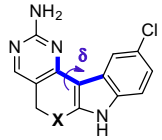

Compound	X	NIK_CLA_IC$_{50}$[20] (μM)	δ (Dihedral angle, calcd) (°)
23	$-CH_2-$	1.2 (n = 1)	10
21	$-(CH_2)_2-$	0.070	27
24	$-(CH_2)_3-$	21	52

environment. Yet, access to this sizable back pocket appears restricted by a narrow channel formed by M469 and K429.

The dihedral angle, δ, for compound **25** as determined from the X-ray structure is 10°. Calculations[25] on **25** and the closely related compound, **21**, in the absence of the protein show a preference for a biaryl dihedral angle of 27° (Table 5). The calculated solution phase dihedral angle for compound **23** is 10° in line with the angle for **25** bound to the NIK protein yet the compound is significantly less potent. Modeling suggests that the smaller six-membered ring of **23** results in a shift in the indole position. This causes the Cl atom to be displaced by more than 1 Å as compared to the Br atom in **25** thus yielding interactions which are less favorable for binding. The low energy conformation of compound **24** has a large 52° dihedral angle and would pay a higher energy penalty (>6 kcal/mol) to rotate the biaryl bond as in **25**.

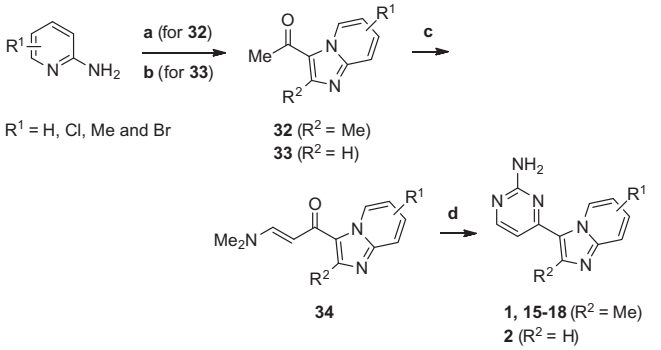

Scheme 1. Reagents and conditions: (a) 3-chloro-2,4-pentanedione, DME, reflux, 60–80%; (b) (i) $Me_2NCH(OMe)_2$, reflux; (ii) bromoacetone, EtOH, 20–40% (two steps); (c) t-$BuOCH(NMe_2)_2$, reflux; (d) guanidine hydrochloride, NaOMe in MeOH, i-PrOH, 85 °C, 70–90%.

Inspired by the co-crystal structure, our efforts then aimed at trying to access this back pocket. The results are summarized in Table 6. Compound **28** proved to be a breakthrough, which exhibited increased activities in both biochemical and cellular assays compared with those of the bromo precursor, **25**. The alkyne linker passes the narrow channel and reaches into the back pocket while the alcohol function potentially assumes the role of a water molecule therein. It appears that both the alcohol functionality and the alkyne linker are essential for activity. The phenyl and thiazole linkers of compounds **29** and **30** are not well tolerated while alkyne-linked pyridine and imidazole of compounds **26** and **27** fail to pick up net positive interactions within the back pocket. These

Table 6
SAR at position 5 of the conformationally constrained indole

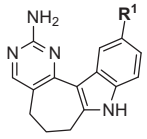

Compound	**25**	**26**	**27**	**28**	**29**	**30**
R^1	Br	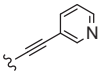	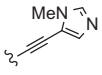			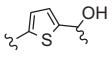
NIK_CLA_IC$_{50}$ (μM)[20]	0.10	30 (n = 1)	30 (n = 1)	0.041	24 (n = 1)	15 (n = 1)
NIK_HT29_IC$_{50}$ (μM)[22]	4.6			0.17		

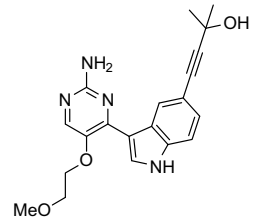

31
NIK_CLA_IC$_{50}$ (μM)[20] 0.040
NIK_HT29_IC$_{50}$ (μM)[22] 0.020

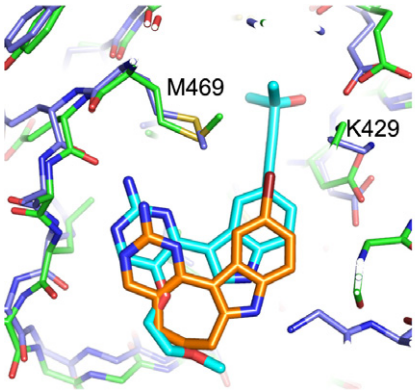

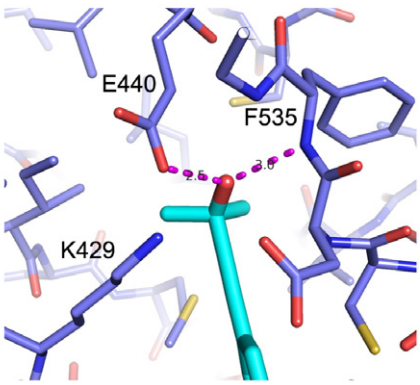

Figure 5. Co-crystals structure of compound **31** with NIK at a resolution of 2.7 Å and its binding site comparison with compound **25** (PDB code: 4IDV.pdb).

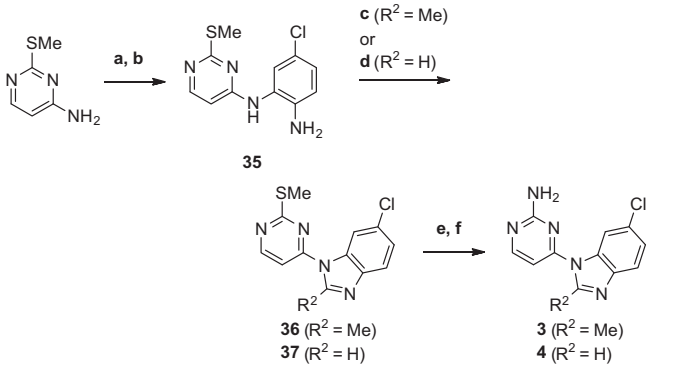

Scheme 2. Reagents and conditions: (a) 2,4-dichloro-1-nitrobenzene, NaH, DMF, 0 °C, 95%; (b) $SnCl_2$ H_2O, EtOAc, reflux, 85%; (c) (i) AcCl, DCM, rt; (ii) TsOH H_2O, toluene, Dean–Stark, 25% (two steps); (d) DMF–DMA, reflux, 80%; (e) *m*-CPBA, DCM, rt; (f) ammonium hydroxide, NH_4Cl, *i*-PrOH, sealed vessel, 100 °C, 20–50% (two steps, not optimized).

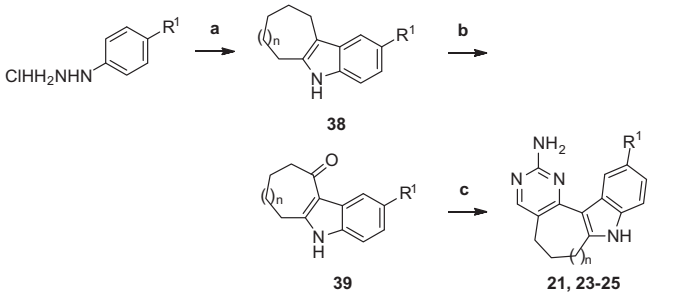

Scheme 3. Reagents and conditions: (a) ketone, glacial AcOH, 140 °C, 95%; (b) DDQ, THF, H_2O, 0 °C to rt, 90%; (c) (i) *t*-BuOCH(NMe_2)$_2$, reflux; (ii) guanidine hydrochloride, NaOMe in MeOH, *i*-PrOH, 85 °C, 85% (two steps).

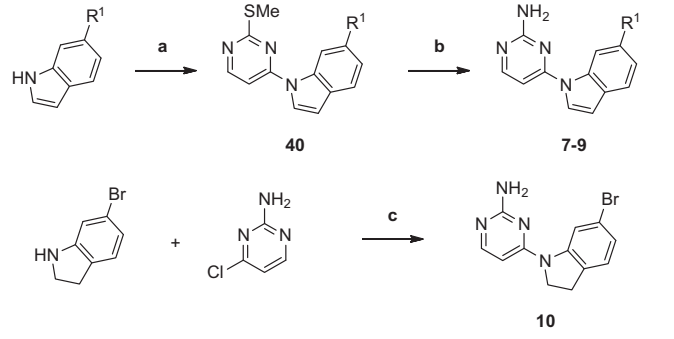

Scheme 4. Reagents and conditions: (a) 4-chloro-2-(methylthio)pyridmine, NaH, DMF, 80 °C, 80%; (b) *m*-CPBA, DCM, rt; (c) ammonium hydroxide, NH_4Cl, *i*-PrOH, sealed vessel, 100 °C, 60% (two steps, R = Br); (d) 1 N HCl (aq), 60 °C, 80%.

results suggest that access to the back pocket helps extend the NIK pharmacophore and thus provides additional binding interactions and boosts potency.

The back-pocket binding was confirmed by the co-crystal structure of compound **31** with NIK (Fig. 5). The alkynyl alcohol interaction pulls the inhibitor deeper into the enzyme binding site as compared with compound **25**. The hydroxyl group makes key H-bonding contacts with E440 and F535 in the back pocket. Furthermore, the co-crystal structure of compound **31** with NIK confirmed that the non-constrained analogs assume conformation **A** in binding.

Compounds were synthesized via the routes outlined in Schemes 1–6. Imidazopyridinyl pyrimidinamines **1**–**2** and **15**–**18** were synthesized as depicted in Scheme 1. Cyclization of 2-pyridinamines with 3-chloropentane-2,4-dione in refluxing 1,2-dimethoxyethane (DME) gave 3-acetyl-2-methylimidazo[1,2-*a*]pyridines **32**,[27] that underwent a facile two-step, one-pot conversion to compounds **1** and **15**–**18** by treatment with Bredereck's reagent and cyclization of the resulting enaminones **34** with guanidine.[23] Compound **2**, which bears no substituent at R2, was synthesized from compound **33** in a similar fashion. Compound **33** was prepared by condensation of 5-bromo-2-pyridinamine with dimethylformamide dimethylacetal followed by treatment with bromoacetone.[28]

Benzimidazolyl pyrimidinamines **3** and **4** were prepared as described in Scheme 2. An SNAr reaction between 2-(methylsulfanyl)-4-pyrimidinamine and 2,4-dichloro-1-nitrobenzene followed by tin reduction of the nitro group furnished aniline **35**.[29] Compound **35** was either treated with acetyl chloride followed by acid-catalyzed cyclization of the resulting amide to give 2-methyl benzimidazole **36**, or treated with dimethylformamide dimethylacetal to give the des-methyl analogue **37**. Oxidation of the methyl sulfides **36** and **37** with *m*-CPBA followed by nucleophilic displacement of the sulfone function with ammonia yielded compounds **3** and **4**, respectively.

Indolyl pyrimidinamine analogs **5**–**6**, **11**–**14**, and **19**–**20** were synthesized in a fashion resembling that used for the guanidine-based indole alkaloids meridianins.[23] The conformationally constrained analogs **21**, **23**–**25** were conveniently synthesized from the corresponding phenyl hydrazines via Fisher indole synthesis followed by oxidation using DDQ[30] and a two-step-in-one-pot formation of the aminopyrimidine ring (Scheme 3). The alkyne and biaryl derivatives of **26** to **30** were obtained either by Sonogashira coupling, as in the synthesis of **31** (Scheme 5), or Suzuki coupling between the bromo precursor **25** and the corresponding alkynes or aryl boronic acids/esters.

The syntheses of compounds **7**–**10** are depicted in Scheme 4. SNAr reaction between various 6-substituted indoles and 4-chloro-2-methylthio)pyrimidine led to intermediates **40**, which were converted to the corresponding 2-aminopyrimidines **7**–**9** using the protocol described in Scheme 2. Compound **10** was conveniently prepared by the reaction of 6-bromoindoline and 4-chloro-2-aminopyrimidine promoted in an acidic aqueous medium.

Compound **22** was synthesized according to Scheme 5. Intermediate **41** was synthesized from ethyl 5-chloro-1*H*-indole-2-carboxylate in four steps via acylation, reduction, ester hydrolysis followed by cyclization.[31] Subsequent reduction and decarboxylation[32] furnished intermediate **42**, which was further elaborated following the same protocol as described in Scheme 1 to provide compound **22**.

Compound **31** was prepared via Sonogashira coupling from its bromo precursor **43** (Scheme 6), which was, in turn, conveniently prepared in three steps from 5-bromoindole. Friedel–Crafts chloroacetylation of 5-bromoindole followed by nucleophilic substitution and aminopyrimidine formation[23] furnished compound **43** in an excellent yield.

In summary, starting with an HTS hit and guided by homology modeling, we identified potent, conformationally restricted NIK inhibitors **21** and **25**. Compound **25** was co-crystallized with NIK protein resulting in one of the first reported NIK co-crystal structures which revealed a large back affinity pocket occupied by a few crystallographically resolved water molecules. Alkynyl alcohol **28** allowed access to the back pocket. The hydroxyl function tethered to the core structure via alkyne bypasses the M469 gatekeeper residue to replace the crystallographic water molecules. Additional binding interactions in the back pocket are illustrated in the

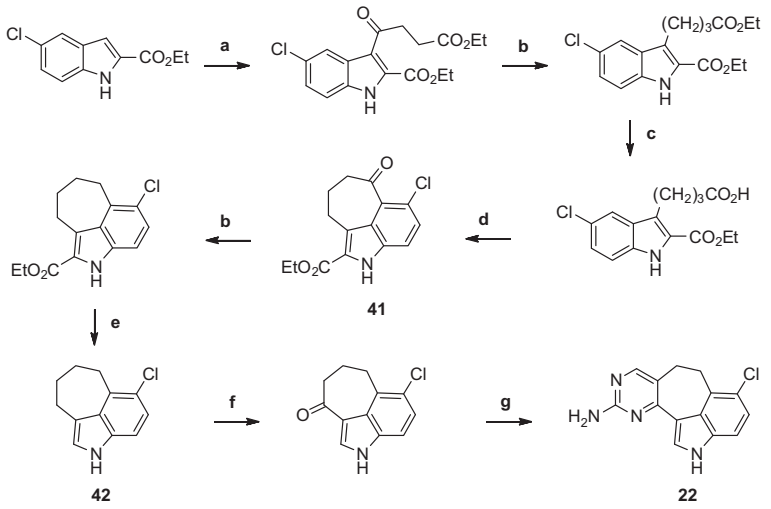

Scheme 5. Reagents and conditions: (a) ethyl 4-chloro-4-oxobutanoate, $AlCl_3$, DCM, 0 °C to rt, 50%; (b) Et_3SiH, TFA, rt, 95%; (c) 30% H_2SO_4, glacial AcOH, 70 °C, 71%; (d) (i) oxalyl chloride, DCM, rt to 40 °C; (ii) $AlCl_3$, DCE, rt to 60 °C, 97% (two steps); (e) (i) LiOH H_2O, MeOH, H_2O, reflux, quantitative; (ii) $Cr_2Cu_2O_5$, quinoline, 200 °C, 85%; (f) DDQ, THF, H_2O, 0 °C to rt, 91%; (g) (i) *t*-BuOCH$(NMe_2)_2$, reflux; (ii) guanidine hydrochloride, NaOMe in MeOH, *i*-PrOH, 85 °C, 85% (two steps).

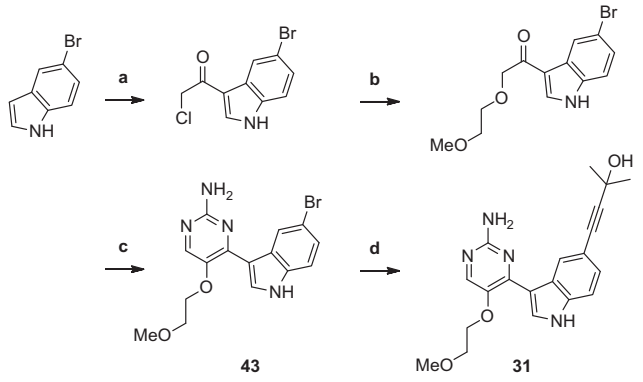

Scheme 6. Reagents and conditions: (a) chloroacetyl chloride, $AlCl_3$, DCM; (b) $MeOCH_2CH_2OH$, NaH, DMF; (c) (i) *t*-BuOCH$(NMe_2)_2$, reflux; (ii) guanidine hydrochloride, NaOMe in MeOH, *i*-PrOH, 85 °C, 85% (three steps); (d) propargyl alcohol, CuI, $Pd(PPh_3)_4$, DMF, 100 °C, 40% (not optimized).

co-crystal structure of another alkynyl alcohol compound **31** with NIK. This work lays the foundation for further optimization efforts towards developing potent and selective NIK inhibitors.

Acknowledgments

The authors thank David Goeddel, Juan Jaen, Marc Labelle, Julio Medina, and Nigel Walker for their scientific discussions, support and encouragement. Xiao He, Zhihong Li, and Holger Wesche are also thanked for their helpful discussions.

References and notes

1. Hayden, M. S.; Ghosh, S. *Cell* **2008**, *132*, 344.
2. Pomerantz, J. L.; Baltimore, D. *Mol. Cell* **2002**, *10*, 693.
3. Dixit, V.; Mak, T. W. *Cell* **2002**, *111*, 615.
4. Xiao, G.; Harhaj, E. W.; Sun, S.-C. *Mol. Cell* **2001**, *7*, 401.
5. Moore, P. A.; Belvedere, O.; Orr, A.; Pieri, K.; LaFleur, D. W.; Feng, P.; Soppet, D.; Charters, M.; Gentz, R.; Parmelee, D.; Li, Y.; Galperina, O.; Giri, J.; Roschke, V.; Nardelli, B.; Carrell, J.; Sosnovtseva, S.; Greenfield, W.; Ruben, S. M.; Olsen, H. S.; Fikes, J.; Hilbert, D. M. *Science* **1999**, *285*, 260.
6. Schneider, P.; MacKay, F.; Steiner, V.; Hofmann, K.; Bodmer, J.-L.; Holler, N.; Ambrose, C.; Lawton, P.; Bixler, S.; Acha-Orbea, H.; Valmori, D.; Romero, P.; Werner-Favre, C.; Zubler, R. H.; Browning, J. L.; Tschopp, J. *J. Exp. Med.* **1999**, *189*, 1747.
7. Thompson, J. S.; Bixler, S. A.; Qian, F.; Vora, K.; Scott, M. L.; Cachero, T. G.; Hession, C.; Schneider, P.; Sizing, I. D.; Mullen, C.; Strauch, K.; Zafari, M.; Benjamin, C. D.; Tschopp, J.; Browning, J. L.; Ambrose, C. *Science* **2001**, *293*, 2108.
8. Yan, M.; Zhang, Z.; Brady, J. R.; Schilbach, S.; Fairbrother, W. J.; Dixit, V. M. *Curr. Biol.* **2002**, *12*, 409.
9. Locksley, R. M.; Killeen, N.; Lenardo, M. J. *Cell* **2001**, *104*, 487.
10. Kalled, S. L. *Curr. Opin. Investig. Drugs* **2002**, *3*, 1005.
11. Mackay, F.; Schneider, P.; Rennert, P.; Browning, J. *Annu. Rev. Immunol.* **2003**, *21*, 231.
12. Saitoh, Y.; Yamamoto, N.; Dewan, M. Z.; Sugimoto, H.; Bruyn, V. J. M.; Iwasaki, Y.; Matsubara, K.; Qi, X.; Saitoh, T.; Imoto, I.; Inazawa, J.; Utsunomiya, A.; Watanabe, T.; Masuda, T.; Yamamoto, N.; Yamaoka, S. *Blood* **2008**, *111*, 5118.
13. Annunziata, C. M.; Davis, R. E.; Demchenko, Y.; Bellamy, W.; Gabrea, A.; Zhan, F.; Lenz, G.; Hanamura, I.; Wright, G.; Xiao, W.; Dave, S.; Hurt, E. M.; Tan, B.; Zhao, H.; Stephens, O.; Santra, M.; Williams, D. R.; Dang, L.; Barlogie, B.; Shaughnessy, J. D., Jr.; Kuehl, W. M.; Staudt, L. M. *Cancer Cell* **2007**, *12*, 115.
14. Keats, J. J.; Fonseca, R.; Chesi, M.; Schop, R.; Baker, A.; Chng, W.-J.; Wier, S. V.; Tiedemann, R.; Shi, C.-X.; Sebag, M.; Braggio, E.; Henry, T.; Zhu, Y.-X.; Fogle, H.; Price-Troska, T.; Ahmann, G.; Mancini, C.; Brents, L. A.; Kumar, S.; Greipp, P.; Dispenzieri, A.; Bryant, B.; Mulligan, G.; Bruhn, L.; Barrett, M.; Valdez, R.; Trent, J.; Stewart, A. K.; Carpten, J.; Bergsagel, P. L. *Cancer Cell* **2007**, *12*, 131.
15. Fu, Y.-X.; Chaplin, D. D. *Annu. Rev. Immunol.* **1999**, *17*, 399.
16. Ramakrishnan, P.; Wang, W.; Wallach, D. *Immunity* **2004**, *21*, 477.
17. Novack, D. V.; Yin, L.; Hagen-Stapleton, A.; Schreiber, R. D.; Goeddel, D. V.; Ross, F. P.; Teitelbaum, S. L. *J. Exp. Med.* **2003**, *198*, 771.
18. Kayagaki, N.; Yan, M.; Seshasayee, D.; Wang, H.; Lee, W.; French, D. M.; Grewal, I. S.; Cochran, A. G.; Gordon, N. C.; Yin, J.; Starovasnik, M. A.; Dixit, V. M. *Immunity* **2002**, *17*, 515.
19. Schrama, D.; Straten, P. T.; Fischer, W. H.; McLellan, A. D.; Bröcker, E.-B.; Reisfeld, R. A.; Becker, J. C. *Immunity* **2001**, *14*, 111.
20. *NIK biochemical chemiluminescent assay (NIK_CLA_IC$_{50}$)*: On a neutravidin precoated plate, compounds in serial dilution were mixed with 10 nM of biotinylated NIK protein and 40 mM ATP in assay buffer (20 mM Tris–HCl pH7.5, 40 mM $MgCl_2$, freshly added 1.5 mM DTT). After 1 h incubation at room temperature, the plate was washed in water four times. The auto-phosphorylated NIK proteins were detected by Anti-Ser/Thr-Pro, MPM-2, phospho Antibody (Millipore) plus HRP conjugated anti-mouse IgG secondary antibody in antibody buffer (20% of SuperBlock Blocking Buffer from Thermo Scientific in PBST0.05). SuperSignal ELISA Pico Chemiluminescent Substrate (Thermo Scientific) was used to measure chemiluminescent signal. The IC_{50}'s were marked $n = 1$ for those compounds that were run only once in this assay. The others were averaged values from 2 or more runs with a standard deviation less than 30%. In each run, compounds were assayed in triplicate.
21. Liu, J.; Sudom, A.; Min, X.; Cao, Z.; Gao, X.; Ayres, M.; Lee, F.; Cao, P.; Johnstone, S.; Plotnikova, O.; Walker, N.; Chen, G.; Wang, Z. *J. Biol. Chem.* **2012**, *287*, 27326.
22. *NIK cell based assay—anti-p52 enzyme-linked DNA/protein interaction assay (NIK_HT29_IC$_{50}$)*: HT29 cells were plated in 6-well plate and treated with compounds in serial dilution in a tissue culture incubator for 30 min and then induced with 100 ng/mL Lymphotoxin alphabeta 2 (R&D System) for 5 h. Whole cell lysates were collected and incubated with biotinylated dsOligo containing the NF-κB binding site that was immobilized on neutravidin—coated plate. After 1 h DNA/protein binding at room temperature with gentle agitation, the plate was washed and NF-κB p52 antibody (Millipore) was added followed by an HRP conjugated secondary antibody incubation. The NF-κB p52

protein level was measured using SuperSignal ELISA Pico Chemiluminescent Substrate (Thermo Scientific). The IC_{50}'s were averaged values from 2 or more runs with variations less than two fold. In each run, compounds were assayed in triplicate.
23. Fresneda, P. M.; Molina, P.; Bleda, J. A. *Tetrahedron* **2001**, *57*, 2355.
24. Zhao, B.; Bower, M. J.; McDevitt, P. J.; Zhao, H.; Davis, S. T.; Johanson, K. O.; Green, S. M.; Concha, N. O.; Zhou, B. B. *J. Biol. Chem.* **2002**, *277*, 46609.
25. Maestro v9.3, Macromodel v9.9. Schrodigner, LLC; New York, NY. Full conformational search with Macrodel was performed for each molecule in water. Dihedral angle, δ, of the lowest energy conformation is reported. Torsional scan calculations were performed for **5**, **6**, **19** and **20** around the biaryl bond to assess the effects of *ortho* substitution.
26. While this manuscript was in preparation, others published small molecule-bound NIK co-crystal structures. Leon-Boenig, G. D.; Bowman, K. K.; Feng, J. A.; Crawford, T.; Everett, C.; Franke, Y.; Oh, A.; Stanley, M.; Staben, S. T.; Starovasnik, M. A.; Wallweber, H. J. A.; Wu, J.; Wu, L. C.; Johnson, A. R.; Hymowitz, S. G. *Structure* **2012**, *20*, 1.
27. Starrett, J. E., Jr.; Montzka, T. A.; Crosswell, A. R.; Cavanagh, R. L. *J. Med. Chem.* **1989**, *32*, 2204.
28. Hayakawa, M.; Kaizawa, H.; Kawaguchi, K.; Ishikawa, N.; Koizumi, T.; Ohishi, T.; Yamano, M.; Okada, M.; Ohta, M.; Tsukamoto, S.; Raynaud, F. I.; Waterfield, M. D.; Parker, P.; Workman, P. *Bioorg. Med. Chem.* **2007**, *15*, 403.
29. Chakrabarti, J. K.; Hotten, T. M.; Pullar, I. A.; Steggles, D. J. *J. Med. Chem.* **1989**, *32*, 2375.
30. Oikawa, Y.; Yonemitsu, O. *J. Org. Chem.* **1977**, *42*, 1213.
31. Tani, M.; Matsumoto, S.; Aida, Y.; Arikawa, S.; Nakane, A.; Yokoyama, Y.; Murakami, Y. *Chem. Pharm. Bull.* **1994**, *42*, 443.
32. Menciu, C.; Duflos, M.; Fouchard, F.; Baut, G. L.; Emig, P.; Achterrath, U.; Szelenyi, I.; Nickel, B.; Schmidt, J.; Günther, B.; Kutscher, E. *J. Med. Chem.* **1999**, *42*, 638.